THE JOURNAL OF COMPARATIVE NEUROLOGY 466:564–576 (2003)

Extraordinary Diversity in Vasopressin (V1a) Receptor Distributions among Wild Prairie Voles (*Microtus ochrogaster*): Patterns of Variation and Covariation

STEVEN M. PHELPS[1]* AND LARRY J. YOUNG[1,2]
[1]Center for Behavioral Neuroscience, Emory University, Atlanta, Georgia 30322
[2]Department of Psychiatry and Behavioral Sciences, Emory University, Atlanta, Georgia 30322

ABSTRACT

The vasopressin V1a receptor is a gene known to be central to species differences in social behavior, including differences between the monogamous prairie vole and its promiscuous congeners. To examine how individual differences compare with species differences, we characterize variability in the expression of the vasopressin V1a receptor (V1aR) in a large sample of wild prairie voles. We find a surprising degree of intraspecific variation in V1aR binding that does not seem attributable to experimental sources. Most brain regions exhibit differences between upper and lower quartiles that are comparable to differences between species in this genus. Regions that are less variable have been implicated previously in regulating monogamous behaviors, suggesting that the lack of variation at these sites could reflect natural selection on mating system. Many brain regions covary strongly. The overall pattern of covariation reflects the developmental origins of brain regions. This finding suggests that shared mechanisms of transcriptional regulation may limit the patterns of gene expression. Such biases may shape both the efficacy of selection and the pattern of individual and species differences. Overall, our data indicate that the prairie vole would be a useful model for exploring how individual differences in gene expression influence complex social behaviors. J. Comp. Neurol. 466:564–576, 2003.

Indexing terms: affiliation; neuropeptide receptor; individual differences; monogamy; evolution; phenotypic correlations

Evolutionary biologists have long known that the rate at which a trait evolves depends not only on the value of possessing that trait, but on several factors that reflect the details of how a trait is implemented. The complex interaction of gene products that produce a trait, the heritability of gene expression, and the involvement of those genes in other traits all contribute to the pace of evolutionary change. In short, the genetic architecture of trait expression shapes its evolutionary potential. It follows that to fully understand the origins of behavioral diversity, one needs to characterize the extent and pattern of variation in gene expression profiles that mediate particular behaviors. Because hormonal and neuromodulatory systems coordinate the expression of complex behaviors, they make excellent models for understanding the contributions of individual genes to behavioral evolution.

One such model system is arginine vasopressin (AVP) and the vasopressin V1a receptor (V1aR), a neuromodulatory system that has been widely implicated in the regulation of vertebrate social behaviors (Young, 1999; Goodson and Bass, 2001). Vasopressin and its nonmammalian homologue vasotocin are modulators of species-specific be-

Grant sponsor: National Science Foundation; Grant number: IBN-9876754 (S.M.P.); Grant sponsor: National Institute of Mental Health; Grant number: MH056897 (L.J.Y.).

*Correspondence to: Steven M. Phelps, Department of Zoology, University of Florida, Gainsville, FL 32611. E-mail: phelps@zoo.ufl.edu

Received 19 February 2003; Revised 30 June 2003; Accepted 2 July 2003
DOI 10.1002/cne.10902
Published online the week of October 6, 2003 in Wiley InterScience (www.interscience.wiley.com).

haviors, including social recognition (Englemann and Landgraf, 1994), social communication (Boyd, 1994; Goodson, 1998; Goodson and Bass, 2000), aggression (Ferris et al., 1997; Goodson, 1998), scent marking (Ferris et al., 1984), paternal care (Wang et al., 1994), and the formation of pair-bonds in monogamous species (Winslow et al., 1993). Consistent with the species-specific effects of AVP on behavior, V1aR exhibits remarkable species differences in its neuroanatomic distribution, even among closely related species (Young, 1999). Among microtine rodents, the patterns of V1aR distribution in the brain are associated with social organization (Insel et al., 1994). For example, the monogamous prairie (*Microtus ochrogaster*) and pine voles (*M. pinetorum*) share a common pattern of V1aR distribution that is distinct from their promiscuous congeners, the meadow (*M. pennsylvanicus*) and montane (*M. montanus*) voles. Several observations demonstrate that patterns of V1aR binding in the brain directly influence species-specific social behavior. First, intracerebroventricular injection of AVP into prairie voles facilitates partner preference formation and increases social interactions but has no such effect in the promiscuous montane vole (Winslow et al., 1993; Young et al., 1999a). Second, AVP injections also enhance social affiliation in transgenic mice with a prairie-like V1aR profile, but do not cause these behaviors in wild-type mice (Young et al., 1999a). Finally, increasing V1aR expression in the ventral forebrain of the prairie vole by using viral vectors facilitates pair-bond formation in the absence of mating (Pitkow et al., 2001).

The association between social organization and V1aR distribution extends beyond *Microtus*. For example, the monogamous *Peromyscus californicus* exhibits high levels of V1aR binding in the ventral pallidum compared with the promiscuous *P. leucopus* (Bester-Meredith et al., 1999). Similarly in primates, the monogamous common marmoset has high levels of V1aR binding in the ventral forebrain compared with the nonmonogamous rhesus macaque (Wang et al., 1997; Young et al., 1999b). There are numerous additional species differences in receptor distribution that have yet to be associated with species-typical behaviors.

It seems that an important step toward understanding the evolutionary diversification of social behavior is to characterize the extent and pattern of V1aR variation within natural populations of a single species. It is not clear, for example, whether the emergence of profound differences between congeners emerges during speciation or might reflect a large pool of intraspecific variation that has simply gone undocumented. Investigating the natural history of neuroanatomic variation can provide insight into the emergence of species differences, while offering a novel model of individual differences in social behavior.

Here, we document the extent and nature of variation in V1aR binding in the brains of a wild, free-living population of prairie voles. First, we present the frequency distribution of receptor binding densities within the population for a wide range of forebrain and thalamic structures, some of which show bimodal distributions. We follow this with simple tests for sex differences, taking advantage of a large sample size (32 unmanipulated adults) to characterize naturally occurring differences. Finally, we provide a novel analysis of covariation in specific V1aR binding among brain regions. We use hierarchical clustering methods to describe natural patterns of correlation between structures and assess the validity of these clusters by using bootstrap statistical analyses. The cluster analysis provides a more global synopsis of observed variation, allowing us to determine whether there are any clear patterns in the sorts of structures that are likely to covary. These axes of variation and covariation define the phenotypes upon which selection is able to act. Because V1aR expression is so closely tied to social behavior, examination of such diversity can inform our understanding of the evolutionary diversification of the complex suite of behaviors that comprise social systems.

Abbreviations

AOB	accessory olfactory bulb
C Amyg	central nucleus of the amygdala
GrAOB	granule cell layer of accessory olfactory bulb
Olf Bulb	olfactory bulb
L BST	lateral bed nucleus of the stria terminalis
L Sept	lateral septum
LD Thal	laterodorsal thalamus
M Amyg	medial nucleus of the amygdala
M BST	medial bed nucleus of the stria terminalis
M Gen	medial geniculate
MD Thal, L	lateral mediodorsal thalamic nucleus
MD Thal, M	medial mediodorsal thalamic nucleus
P Cing	posterior cingulate cortex
V BST	ventral portion of lateral and medial bed nucleus of the stria terminalis
V Pall	ventral pallidum
VP Thal	ventral posterior thalamic nucleus

MATERIALS AND METHODS

Animal subjects

Male and female prairie voles were caught in and around Champaign, Illinois, by using Sherman Live Traps (3 inches × 3.5 inches × 9 inches) baited with cracked corn. Traps were checked twice daily for captures. Animals were weighed, sexed, and examined for several morphologic features used to identify the species caught. Animals that were clearly microtine rodents were assigned to the species prairie vole based on three initial criteria: a tail shorter than 37 mm, a reddish hue to the venter, and the presence of five toe pads (Hofmeister, 1989). Animals that seemed ambiguous in any of these features were assessed for the number of cuspids in the third upper molar, a definitive morphologic feature distinguishing prairie voles from their sympatric congener, the meadow vole, *Microtus pennsylvanicus* (Hofmeister, 1989). Analysis of molars revealed no species misidentifications.

Animals were euthanized by CO_2 asphyxiation, the brains were removed and stored on dry ice and shipped to Emory University where they were stored at −70°C until processing. Gonads were dissected to confirm reproductive condition of the animals. A total of 18 males and 14 females were caught. All animals were reproductively mature. Animal protocols were approved by the IACUC committee at Emory University.

Radioligand receptor autoradiography

Brains were sectioned on a cryostat at a thickness of 20 μm. Coronal sections were taken every 100 μm, beginning in the olfactory bulb and extending caudally past the level of the ventroposterior thalamus, stopping at approximately the level of the medial geniculate and superior

colliculus. Slides were allowed to dry at room temperature during the slicing, and then were stored at −70°C until autoradiographic binding was performed.

Receptor autoradiography was performed by using ^{125}I-labeled linear vasopressin V_{1a} receptor ligand (HO-phenylacetyl^{1}-*D*-Tyr(Me) ^{2}-Phe^{3}-Gln^{4}-Asn^{5}-Arg^{6}-Pro^{7}-Arg^{8}-NH2, Perkin-Elmer Scientific [NEX-310]) as described previously (Young et al., 1997). The sections were pretreated with 0.1% paraformaldehyde in phosphate-buffered saline (pH 7.2) for 2 minutes at room temperature. After a prewash in 50 mM Tris-HCl (pH 7.4), slides were exposed to a 60-minute room temperature incubation of 50 pM ^{125}I-antagonist in 50 mM Tris with 10 mM $MgCl_2$ and 0.1% bovine serum albumin (radioimmunoassay grade, fraction V; Sigma, St. Louis, MO). The binding buffer was made in sufficient volume that all sections were incubated simultaneously using the same buffer, removing variation in binding buffer as a source of variation in binding. Unbound ligand was removed by four washes in 50 mM Tris, pH 7.4, 100 mM $MgCl_2$. After air-drying, the slides were exposed to BioMax MR film (Kodak, Rochester, NY) along with ^{125}I-labeled autoradiographic standards for 68 hours.

After film exposure, slides were counterstained for acetylcholinesterase and used to identify landmarks needed to delineate neuroanatomic boundaries. Neuroanatomic boundaries were defined by using a rat brain atlas (Paxinos and Watson, 1998) and are summarized in Figure 1.

Data analysis

Optical density readings were measured and converted to decompositions per minute (dpm)/milligram tissue equivalent (TE) based on autoradiographic standards using the NIH Image software (available free at http://rsb.info.nih.gov/nih-image). Each brain region was measured bilaterally in at least three sections 100 μm apart, and the average of the six readings was recorded. Specific binding for a given region was calculated by subtracting the mean density of nonspecific binding in an adjacent region of cortex from the mean binding density in the region of interest. Individual differences in specific binding are reported in Figure 2, which displays histograms for many of the regions investigated.

Analysis of covariation

Before examining patterns of covariation across brain regions, we first regressed "whole-brain–specific binding" against each individual region. Variation in tissue quality could conceivably lead to variation in binding that would lead to positive correlations in many structures; the residuals of these regressions represent binding that is not attributable to variation in whole-brain binding. Whole-brain binding was defined as the sum of the total specific binding measured in the brain regions investigated. After statistically controlling for whole-brain binding, we calculated pair-wise correlations between regions. Using the regression residuals reduced the strength of positive correlations between many regions and revealed negative correlations between many others, but did not change the hierarchical pattern of the correlations. We do not report the exact values or significance levels of individual correlations because they were not used in hypothesis testing.

We transformed the correlation matrix into a distance matrix simply by defining distance as 1-r, where r is the Pearson correlation coefficient. Distances were thus maximal (near 2.0) when correlations were strong and negative, and minimal (near 0.0) when correlations were strong and positive. The resulting distance matrix was used to perform a hierarchical cluster analysis.

Hierarchical cluster analysis is a means of visualizing the similarity between variables. The distance matrix is first used to determine which pair of variables are least distant; these two variables are joined into a cluster, and the distances between the cluster and all other variables are calculated, resulting in a new distance matrix in which the new cluster replaces its component variables. This procedure is done iteratively until all variables are joined into a single cluster. (For convenience, we refer to the complete set of clusters as a tree or dendrogram.) In general, which clusters are formed and how they are interpreted vary somewhat with the criteria used to calculate the distance matrix from the original data, and with the method used to calculate distances between new clusters and the remaining variables. In our analysis, the distance at which a cluster is formed represents the mean distance between members of the cluster. A cluster formed at a distance $d = 0.25$, for example, would be composed of a series of brain regions that have an average pair-wise correlation coefficient of $r = 0.75$; a cluster joined at a distance of 1.75 would have an average $r = -0.75$. In our analysis, distance represents both the strength and sign of the correlations between the clustered brain regions.

Bootstrap analysis of cluster results

To assess the stability of cluster results, it is necessary to use simulation methods to resample the original data set and estimate the frequency of each cluster in the resulting sample of trees. Brown (1994) reviews three types of hypothesis tests that can be performed on dendrograms, including but not limited to trees produced by hierarchical cluster analysis.

The first, type I, is a test that assesses whether a given cluster is significantly more likely to occur in a resampling of the data than in a null data set. The null data set is defined to be one in which the distributions of individual variables are identical to those of the original data sample, but in which the variables are independent of one another. This strategy is executed by drawing individuals with replacement from the original data set, yielding a new data set with an identical number of individuals. A null data set is constructed from this bootstrapped data by randomly reassigning a variable's entries to different individuals. This permutation of the data preserves the distributions of each variable, but makes all variables independent. The cluster analysis is then performed on both the bootstrapped data and the null data. Both trees are surveyed to see if a particular cluster is present. If one tree displays the cluster but the other does not, this iteration of bootstrapping is considered informative and scored. New bootstrapped and null data sets are generated until a desired number of informative samples have been obtained. The probability that the cluster is more likely in the bootstrapped data than in the null data is computed using a sign-test. Because several mutually exclusive clusters can be supported over those gleaned from null data, this approach represents the weakest of the three tests Brown (1994) outlined.

The second class of test (Brown's type II) directly compares the support for one grouping over another grouping. To perform this test, a bootstrapped data set is constructed and the resulting tree assessed for the presence

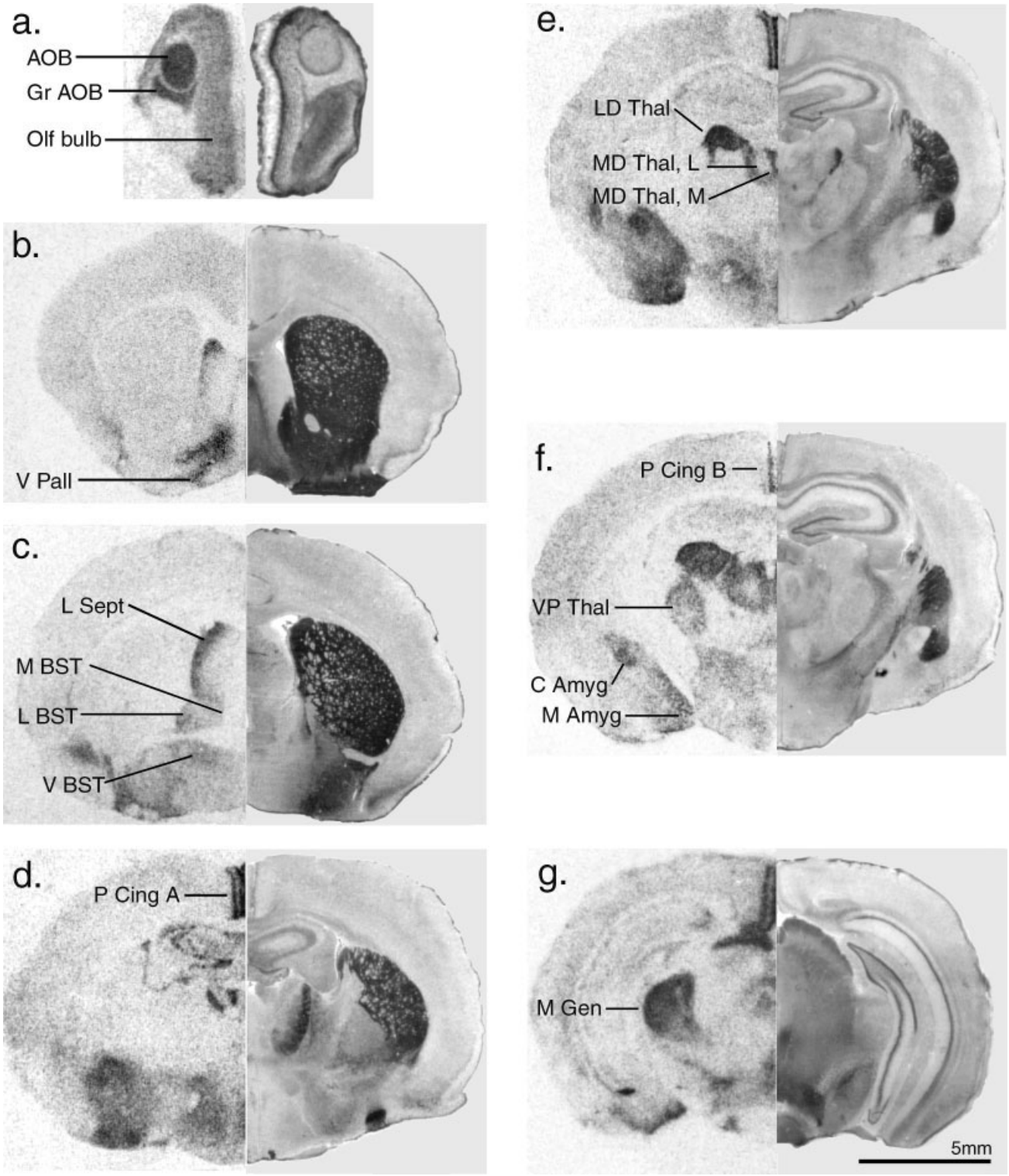

Fig. 1. **a–g:** Regions in which vasopressin V1a receptor (V1aR) binding was measured. Sections are arranged in rostral (a) to caudal (g) order. The left side of each panel is an autoradiography film; the right side is a matching section stained for acetylcholinesterase and counterstained with cresyl violet. The sections are not necessarily from the same brain. Panels in this figure have been adjusted for brightness and contrast by using Adobe Photoshop version 6.0. For abbreviations, see list. Scale bar = 5 mm in g (applies to a–g).

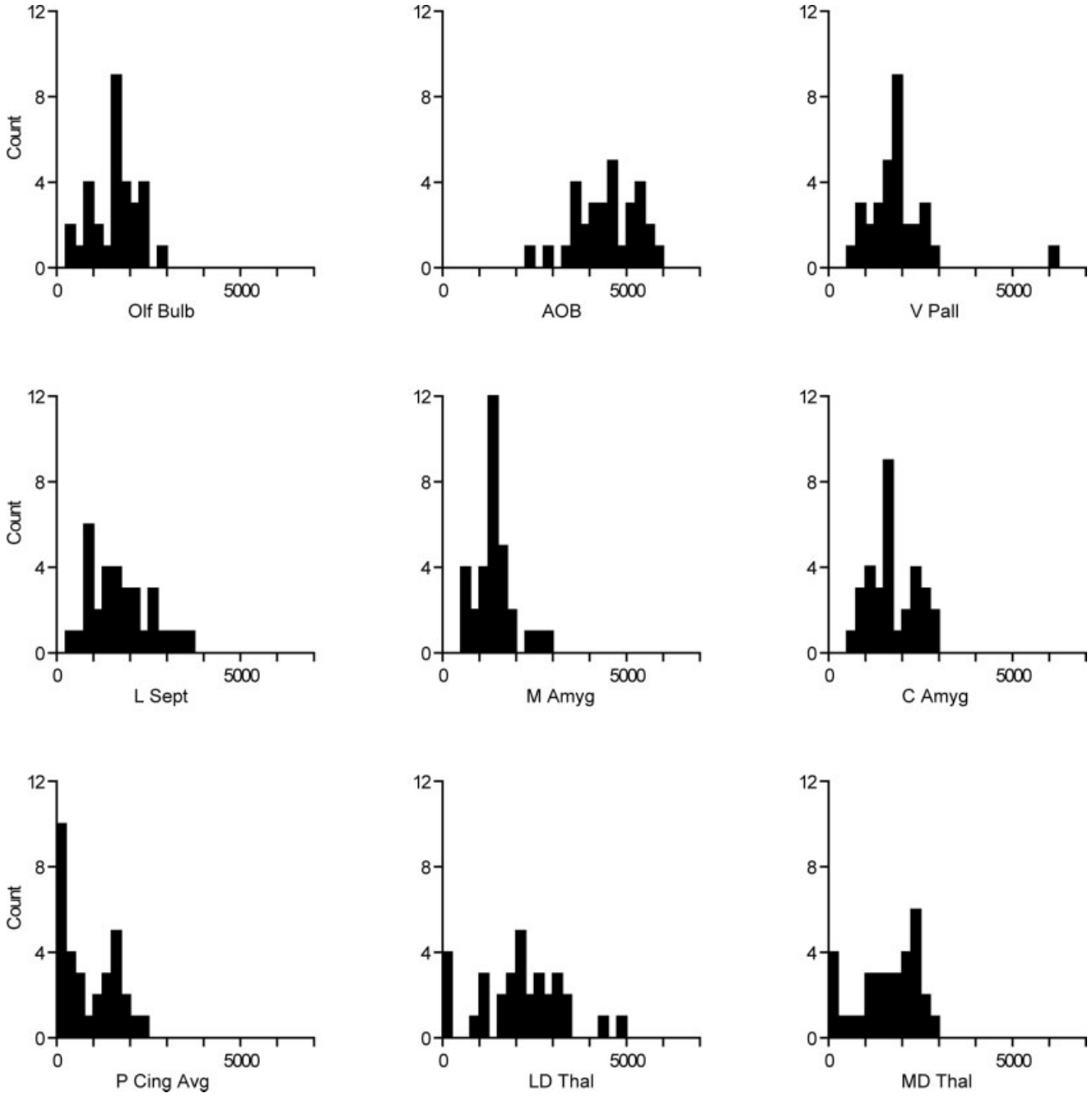

Fig. 2. Histograms summarizing individual differences in nine of the brain regions measured. Binding density is measured in disintegrations per milligram of tissue equivalents. Note that closely related brain regions that were measured separately for the purposes of examining patterns of covariation (P Cing A and B, and MD Thal L and M; see Materials and Methods for details) have been pooled here. For abbreviations, see list.

of one of two mutually exclusive clusters. If one of the clusters is present, the iteration is informative. Again the bootstrap procedure is repeated until a desired number of informative replicates has been obtained. The probability that one cluster is more likely than a second is computed using a sign-test. We used this test to compare the support for a cluster obtained from our original analysis to that of a cluster predicted a priori from the proximity of different regions on a slide. This test allows us to directly assess whether our clusters could be explained as by-products of between-section variation in binding.

We report a novel modification of the type II test that allows one to assess whether a given cluster is the most supported of all possible alternatives. In this procedure, we generate bootstrapped data sets and record the presence or absence of the cluster in question. If the cluster is

TABLE 1. Individual Differences in V1aR Binding[1]

	Quartile boundaries			Sex comparisons (n = 14 females, 18 males)			Individual vs. species diffs	
Region	Low	μ	High	Female ± std	Male ± std	*P*	Indiv	Species
AOB	3742	4456	5142	4305 ± 757	4580 ± 927	0.37	1.37	—
BST, L	474	781	989	717 ± 232	831 ± 715	0.53	2.09	1.80*
BST, M	125	307	460	358 ± 180	268 ± 257	0.26	3.68	—
BST, V	681	1286	1645	1245 ± 612	1318 ± 1162	0.82	2.41	1.83*
C Amyg	1236	1733	2365	1781 ± 683	1695 ± 599	0.71	1.91	3.14*
Gr AOB	2815	3465	4019	3379 ± 681	3536 ± 975	0.60	1.43	—
L Sept	977	1750	2286	1728 ± 642	1767 ± 956	0.89	2.34	2.67*
LD Thal	1492	2092	3078	1987 ± 1232	2175 ± 1204	0.67	2.06	7.30*
M Amyg	1186	1436	1660	1571 ± 547	1331 ± 439	0.19	1.40	1.17
MD Thal (Avg)	1033	1575	2273	1576 ± 978	1574 ± 804	0.99	2.20	1.69*
MD Thal, L	901	1641	2388	1614 ± 1002	1661 ± 890	0.89	2.65	—
MD Thal, M	946	1510	2236	1539 ± 973	1487 ± 756	0.87	2.36	—
M Gen	182	1502	2206	1515 ± 919	1492 ± 1394	0.96	12.12	1.37
Olf Bulb	989	1595	2022	1575 ± 617	1612 ± 652	0.87	2.05	—
P Cing (Avg)	157	873	1602	979 ± 728	791 ± 758	0.48	10.19	2.36
P Cing A	153	810	1425	886 ± 626	751 ± 748	0.58	9.31	—
P Cing B	180	937	1846	1072 ± 887	832 ± 812	0.44	10.25	—
V Pall	1314	1903	2218	1790 ± 623	1991 ± 1173	0.54	1.69	1.51*
VP Thal	0	597	975	789 ± 661	447 ± 662	0.16	>10.00	3.87*

[1]Quartile boundaries: Low quartile boundaries represent the level of V1aR binding (dpm/mg TE) of the eighth lowest of 32 subjects, μ the mean, and High the eighth highest binding. Sex comparisons: Female ± std represents the mean binding for females (n = 14) ± standard deviation, Male ± std the mean male binding (n = 18) ± standard deviation. The reported *P* values correspond to *t*-tests assuming unequal variance, with no corrections for multiple comparisons. Note that the smallest *P* values are 0.16 (VP Thal) and 0.19 (M Amyg), suggesting a general absence of sex differences. Individual vs. species diffs: Indiv is defined as the ratio of the upper and lower quartile boundaries for each brain region (High/low). (Because the lower quartile boundary for the VP Thal is zero, we enter its ratio as ">10.") To calculate a similar metric for species differences, we looked at the means reported for prairie and montane voles in Wang et al. (1997). Species is defined as the larger of the two means divided by the smaller of the two. Asterisks denote species differences that were statistically significant at the $P < 0.05$ level in Wang et al. (1997). The — symbol refers to brain regions that were not reported in comparable terms in Wang et al. (1997). Note that we consider V Pall to be the structure Wang et al. referred to as the diagonal band. V1aR, vasopressin V1a receptor. For other abbreviations, see list.

absent, a list is made of all alternative clusters containing one or more of the variables from the original cluster. We repeat the bootstrap iterations until the frequency of the two most common clusters sum to obtain the desired number of informative replicates. We use a sign-test to compare the support for the most frequent and second most-frequent clusters. If the original cluster is the most frequent, and if it is more strongly supported than the second most-frequent cluster, it follows that the original is more likely than any single alternative.

The third test Brown describes is the most conservative. It tests whether a given cluster is more likely than all other alternatives combined. In this test, the bootstrapped data are scored as either possessing or lacking the cluster in question. Because all trees contain either the hypothesized cluster or a mutually exclusive alternative, all iterations of the bootstrap procedure are informative. The support for the cluster over all possible alternatives combined is computed using a sign-test.

Our analysis consisted of 17 variables joined together in 15 clusters. (The 16th cluster is simply the set of all variables, and so has no alternatives.) To minimize the number of tests performed, we began by assessing each cluster with the most conservative test. Those that failed a conservative test were tested with the next most conservative. Bonferroni corrections of the alpha level were made for multiple tests. The number of informative bootstrapped samples was set to 100, the desired alpha level to 0.05. We first tested all 15 clusters on independently bootstrapped samples to see which of the clusters were more strongly supported than all alternatives combined, correcting the alpha level to 0.003 (0.05/15 = 0.0033). Of these 15 clusters, 6 were significantly more supported than all alternatives combined ($P < 0.003$). The nine that were not supported were tested to determine whether each cluster was significantly better than any single alternative, with an alpha level now set to 0.002 (0.05/24). Of these, six were not supported over every alternative. These six were tested to determine whether they were more likely than clusters drawn from the null samples ($\alpha = 0.05/30 = 0.0016$). For each of these statistics, any observed cluster with $\alpha < P < 0.05$ is considered a non-significant trend. We consider this series of tests and Bonferroni corrections to be a conservative analysis of our data.

Programs for the bootstrap analyses were written by the authors and implemented within the MatLab programming environment. Academic researchers wishing to use the software for comparable analyses should contact SMP for free copies of the source code.

RESULTS

Individual differences in forebrain V1aR binding

Despite the large sample size, there were no significant sex differences in the binding of any of these regions ($P > 0.10$; Table 1), even using the most liberal statistics (single *t* tests, uncorrected for multiple comparisons). This finding is consistent with reports that prairie V1aR expression is generally insensitive to the influence of gonadal hormones (Cushing et al., 2003; Wang, personal communication) and suggest that nongonadal mechanisms must be responsible for individual differences. The data were pooled across sexes for further analysis.

Histograms illustrating the distribution of binding densities for most brain regions analyzed are presented in Figure 2. As one might expect, the variation in many regions was unimodal, with every subject showing a mean binding greater than zero. Among the regions displaying unimodal (one-peaked) distributions (all telencephalic structures except posterior cingulate cortex [P Cing] and perhaps central nucleus of the amygdala [C Amyg]), some regions displayed little variation (ventral pallidum [V Pall], M Amyg) while others displayed substantially more

variation (lateral septum [L Sept]). Perhaps more striking is the finding that many brain regions showed a profound, bimodal (two-peaked) pattern of variation. Such a discrete pattern of variation could correspond to alternative behavioral phenotypes. The P Cing, for example, displayed binding at background levels in at least 30% of the subjects; a second mode occurs near 1,500 dpm/mg TE. Similarly, in each thalamic structure 10–30% of the individuals exhibited specific binding at background levels (<250 dpm/mg TE above background). In laterodorsal thalamus (LD Thal), four subjects lacked binding, with a second mode of six animals displaying approximately 1,250 dpm/mg TE. The same four subjects that lacked binding in the LD Thal lacked binding in the MD Thal, VP Thal, and medial geniculate (M Gen), while having normal binding in several other brain regions (e.g., Fig. 3c). A total of 11 subjects lacked binding in the VP Thal, with a second mode of eight subjects at 1,250 dpm; and seven subjects lacked binding in the M Gen, with a second mode of seven subjects at 2,250 dpm/mg TE. All of the thalamic structures displayed bimodal distributions, with one mode at background and a second nearer the population mean. The C Amyg seemed somewhat bimodal (Fig. 2), but because the distance between the modes is relatively small (1,750 vs. 2,500) and the lower mode is well above background, it is less clear whether this represents discrete variation or sampling error. The bimodal distributions seen in the diencephalon and in the posterior cingulate cortex raises the interesting possibility that there may be discrete behavioral phenotypes associated with each mode.

Sections representing binding in the upper and lower quartile for many of these regions are presented in Figure 3. Similar levels and patterns of variation have been observed within our lab colony (data not shown). We find individuals lacking binding in the P Cing or thalamus while binding in other brain areas is intact. We have not seen an animal from this population lacking binding in either the LD Thal or the MD Thal, without lacking binding throughout the thalamus.

Covariation in binding: Hierarchical clustering, and bootstrap analysis

There were extensive correlations in V1aR binding densities between brain regions. Before correcting for whole-brain–specific binding, pair-wise correlations ranged from −0.24 to +0.89, with a mean correlation coefficient of +0.27 and a median of +0.24. Correcting for variation in whole-brain–specific binding yielded a range of −0.46 to +0.87 (mean = +0.13, median = +0.11, see Fig. 4a), revealing negative correlations that were masked by whole-brain variation and reducing the strength of spurious positive correlations. Despite the change in the size and sign of some correlations, the hierarchical pattern of correlations proved remarkably robust to such transformations, suggesting a general stability of our hierarchical cluster results to various analysis procedures (data not shown). Bootstrapped samples of our data set demonstrate the overall stability of the correlation matrices (Fig. 4b). Null data resulting from breaking the correlations present in corresponding bootstrapped samples revealed no reliable patterns of correlation between regions. All clusters occurred significantly more often in bootstrapped samples than in null samples ($P < 0.001$).

The hierarchical cluster analysis (Fig. 4a) revealed a tight linkage of the AOB and the GrAOB (*distance* $d = 0.16$, supported over all alternatives combined, $P < 0.003$), two functionally and developmentally related structures. This cluster was nested within a general olfactory cluster that includes the main olfactory bulb ($d = 0.39$, represented by the red cluster in Fig. 4a, supported over all alternatives combined, $P < 0.003$).

The lateral and ventral divisions of the bed nucleus of the stria terminalis (BST) clustered with one another ($d = 0.19$, supported over null, $P < 0.001$; not supported over any single alternative, $P > 0.05$), joined first by the ventral pallidum ($d = 0.21$, combined, $P < 0.003$), and then by the medial BST ($d = 0.46$, better than any single alternative, $P < 0.002$). Bootstrap samples often changed the groupings within the cluster {L BST, V BST, V Pall}, but other groupings were extremely stable. We refer to the cluster containing the BST and V Pall brain regions as "pallidal," shown in orange in Figure 4a.

Rostral and caudal measures of the posterior cingulate (A and B, respectively) were joined at a distance of 0.13, despite being separated from one another by ~700 μm and often being located on separate slides (Fig. 4a, combined, $P < 0.003$). The P Cing cluster is joined by the M Amyg at $d = 0.63$ (single alternative, $P < 0.002$). Whereas the P Cing is pallial in origin, the M Amyg derives from the "intermediate zone" adjacent to the pallial anlage; in the laboratory mouse, these structures exhibit overlapping patterns of transcription factor expression (Smith-Fernandez et al., 1998; Puelles et al., 2000).

The pallial/amygdaloid cluster was then joined by L Sept, but this grouping was not reliably observed in our bootstrap analysis (d = 0.77, single alternative, $P > 0.05$). Although the placement of L Sept within this cluster was more likely in the bootstrapped data than in the null data ($P < 0.001$), our results indicate that there were several alternative groupings of the L Sept that were no less likely than the observed grouping (single alternative, $P > 0.05$). Such alternative clusters did reliably place the L Sept within the telencephalon cluster.

The olfactory and pallidal clusters joined at a distance of 0.66, which then joined the cluster consisting of L Sept and the pallium at $d = 0.82$. The deeper groupings within the telencephalic cluster were not observed any more frequently than alternative groupings of these regions ($P > 0.05$). The telencephalon cluster itself was supported over null data ($P < 0.001$) and was favored by a nonsignificant trend when compared with the second most-likely cluster ($P = 0.02$).

The lateral and medial segments of the MD Thal covary strongly and were joined at a distance of 0.15 (combined, $P < 0.003$). These join with the LD Thal at a distance of 0.24 (combined, $P < 0.003$). Surprisingly, these are joined by C Amyg ($d = 0.77$), but this cluster is not significantly supported over the second most likely alternative, a thalamic cluster that includes VP Thal but excludes C Amyg {LD Thal, MD Thal M, MD Thal L, VP Thal} (single alternative, $P = 0.04$). VP Thal and M Gen are joined at a distance of 0.56 (NS single alternative, $P > 0.05$). A deep cluster is then formed {D Thal, MD Thal L,M, VP Thal, M Gen, C Amyg} that consists of all investigated diencephalic structures together with C Amyg ($d = 0.84$). This "diencephalic" cluster was supported over null groupings ($P < 0.001$) but was not significantly better than the second-best alternative ($P > 0.05$). The final cluster, then, consists of joining the telencephalic regions (main and

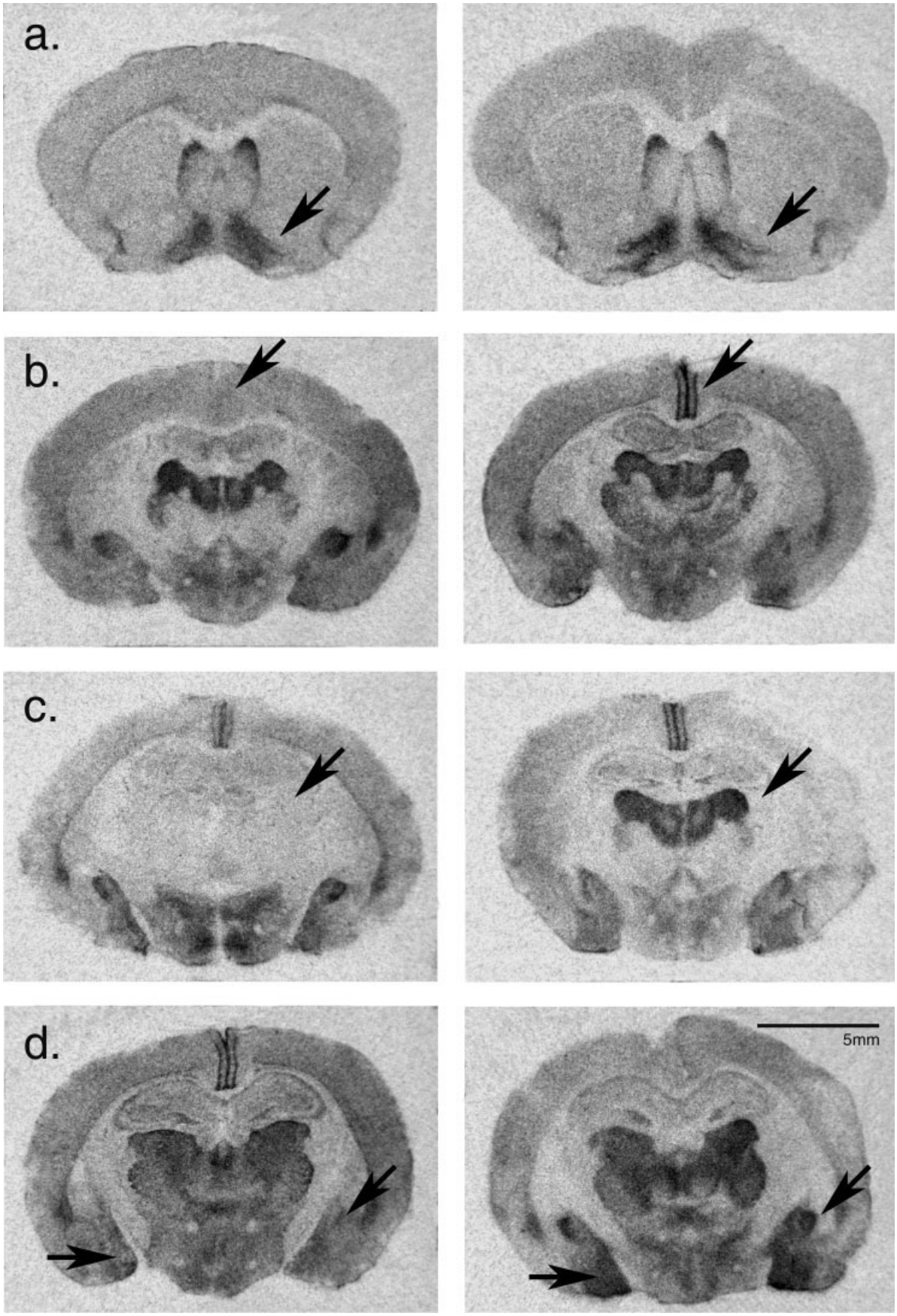

Fig. 3. Representative sections from prairie vole brains in the lower (left) and upper (right) quartiles of vasopressin V1a receptor (V1aR) binding. Arrows indicate the regions illustrated in each pair of panels: ventral pallidum (**a**), posterior cingulate (**b**), laterodorsal and mediodorsal thalamus (**c**), and central and medial amygdala (**d**). Anatomic boundaries used for each of these structures are illustrated in Figure 1. The depicted sections underwent uniform adjustments of brightness and contrast by using Adobe Photoshop version 6.0 software. Scale bar = 5 mm in d (applies to a–d).

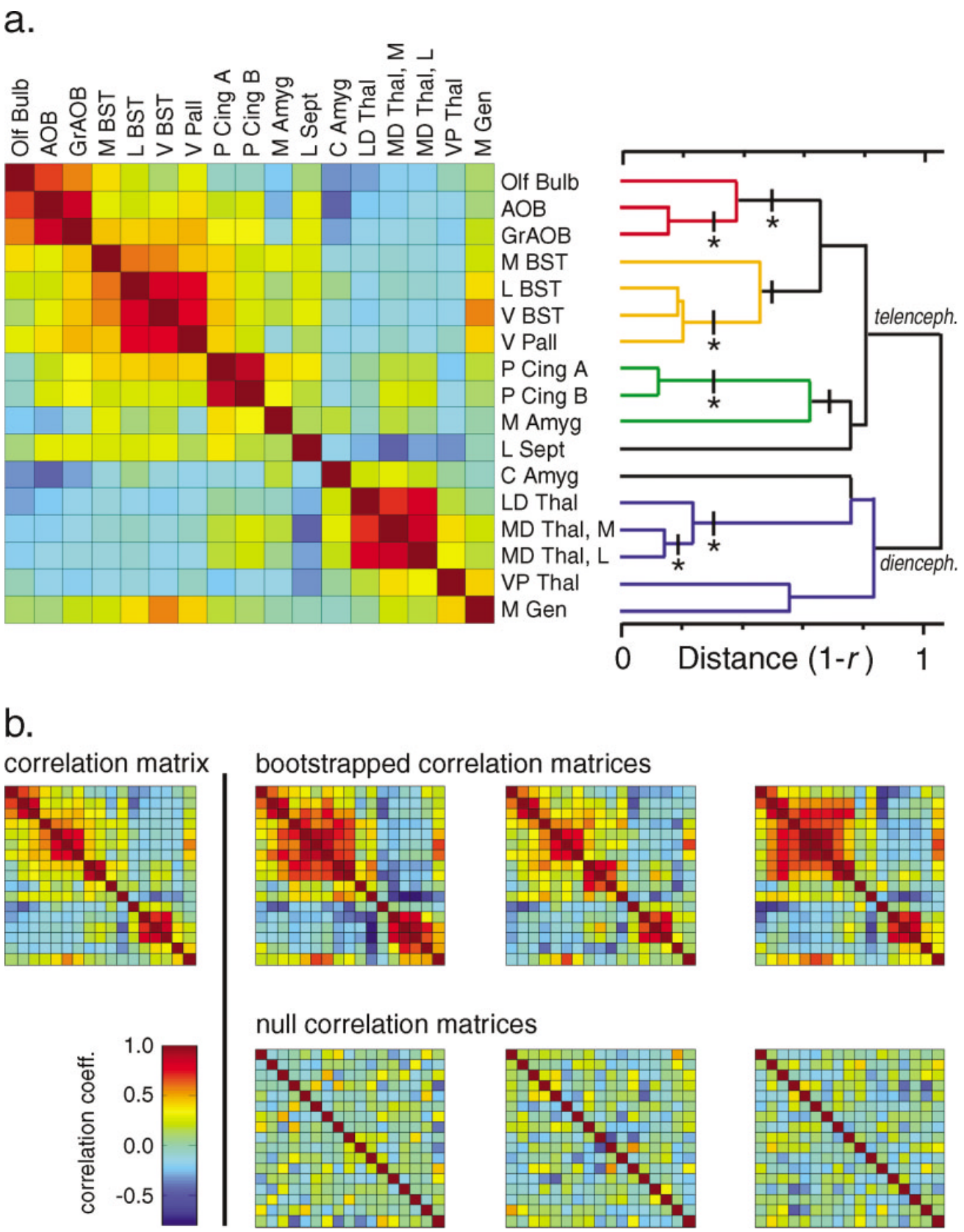

Fig. 4. Patterns of covariation among brain regions exhibiting vasopressin V1a receptor (V1aR) binding. **a:** The left panel is a correlation matrix produced by estimating pair-wise correlation between brain regions following the removal of "whole-brain–specific binding" (see Materials and Methods for details). The color scale is given in Figure 4b. The right panel denotes the hierarchical cluster generated for the data. All clusters were supported over null data ($P < 0.002$, see Fig. 4b, Results section). Clusters with cross-bars were significantly more likely any other cluster (single alternative, $P < 0.002$). Clusters with cross-bars and asterisks were significantly more likely than all alternative clusters combined ($P < 0.003$). **b:** Examples of correlation matrices generated by bootstrap analyses. The upper series depicts the original matrix (left) and three matrices generated by re-sampling individuals with replacement. Note the similarities in the overall patterns of correlations. The lower series depicts the scale used for all matrices in Figure 4 (left), and three "null" matrices generated by randomly re-sampling data for each brain region independently of the individual the region was measured in. Note that the correlations in the null matrices show no hierarchical patterns and have a mean near zero. For abbreviations, see list.

accessory olfactory bulb, pallidum, pallium, and L Sept) with the diencephalon and C Amyg ($d = 1.06$).

Between-section variation is not sufficient to explain observed clusters

If there exist significant procedural sources of between-section variability, regions that are measured on the same section would tend to be correlated and clusters could reflect artifacts of tissue preparation and binding procedures. We minimized this variation by preparing a common binding buffer containing the appropriate concentration of ^{125}I-labeled linear-AVP. Fortunately, we can make a series of a priori predictions for clusters that would emerge as a result of proximity alone. We tested the support for the observed clusters versus artifactual, proximity-based clusters with our bootstrap analysis.

The lateral and medial divisions of the bed nucleus were measured at the same level, a level that included the lateral septum. In our cluster analysis, the lateral and ventral BST clustered with the more rostrally measured V Pall (Fig. 1). We compared the support for the observed cluster {L BST, V BST, V Pall} with that of a predicted proximity-based cluster {L BST, V BST, M BST} and found that the originally observed cluster occurred significantly more often than did the cluster of adjacent BST subdivisions (91 of 100 informative bootstrapped samples, $P < 0.001$). Indeed, the observed cluster was significantly more likely than all other clusters combined ($P < 0.003$), which would include any clustering of its members with the adjacent L Sept.

The posterior cingulate cortex was measured at two levels, termed A and B (Fig. 1). Level B occurred on the same sections that were used to measure binding in the VP Thal, M Amyg, and C Amyg. In fact, the distance between P Cing A and B was ~700 μm, and the two were often on separate slides. A clustering based on between-section variability would join P Cing B with the VP Thal, C Amyg, or M Amyg. In every bootstrapped sample assessed, however, P Cing A and P Cing B always formed a cluster (100 of 100, combined, $P < 0.003$). Despite the distance between these measurements, the correlation between P Cing A and B was stronger than that observed between any other pair ($r = 0.87$).

At the level of the thalamus, the MD and LD Thal are on the same sections and the VP Thal, C Amyg, and M Amyg were slightly caudal. The M Gen, in contrast, was typically ~900 μm caudal to the VP Thal. We compared the observed cluster {VP Thal, M Gen} with the artifactual cluster {VP Thal, C Amyg}. We found the observed {VP Thal, M Gen} to be much more likely than the artifactual cluster {VP Thal, C Amyg} (99 of 100 informative bootstrapped samples, $P < 0.001$).

Because the Olf Bulb, AOB, and GrAOB are adjacent, as well as functionally and developmentally related, the clustering of these three regions could be attributed either to biological or procedural sources of variation. However, if the correlations across these regions are due to section variability, there is no reason to predict any particular pair-wise clustering of these regions. Yet the AOB and GrAOB covary strongly ($r = 0.84$). The observed cluster {AOB, GrAOB} is significantly more likely than all other alternative clusters combined ($P < 0.003$), including the possible pairs {Olf Bulb, GrAOB} and {Olf Bulb, AOB}.

Observed clusters within every major grouping—the olfactory, pallidal, pallial and thalamic clusters—clearly preclude clusters based on between-section variability. The bootstrap analysis refutes between-section variability as an adequate explanation for the hierarchical cluster results.

DISCUSSION

We found a surprising level of variation throughout the prairie vole forebrain. For most regions, the intensity of binding in the upper quartile of individuals was at least twice that of the binding observed in the lower quartile (Table 1). In the M Gen, P Cing, and VP Thal, individuals in the upper quartile had levels of binding that were at least 10-fold greater than those in the lower quartile (Table 1). For the 11 structures in which comparable measures were taken in both our study and that of Wang et al. (1997), only two structures showed higher mean species differences than the differences we report within prairie voles (Table 1). Given that species differences in V1aR contribute to species-typical social behaviors, it seems likely that intraspecific variation in V1aR binding will contribute to individual differences in social behaviors. Structures showing some of the lowest levels of variation (e.g., V Pall, M Amyg) have been implicated in species-specific patterns of pair-bonding and paternal care (Kirkpatrick et al., 1994a, b; Pitkow et al. 2001; Phelps et al., 2002); low variation may reflect selection favoring the expression of these behaviors.

Of interest, those structures showing the most profound individual differences are among the least studied in the context of sociality. The posterior cingulate, for example, is known to be involved in spatial reference memory, presumably through its interactions with the hippocampus and the laterodorsal thalamus (Cooper et al., 2001; Whishaw et al., 2001). Perhaps V1aR variability in the P Cing and LD Thal influences the ability of these animals to recall the spatial position of social cues—an ability that would be useful for the dampening of aggression toward familiar individuals along familiar borders (the "dear enemy" effect), to locating preferred mates for extra-pair copulations, and other sociosexual interactions that can be expected to take place in a natural setting. To our knowledge, no studies have investigated a role for either structure in social behaviors. Similarly, the mediodorsal thalamus, with its input from the ventral pallidum and its output to the prefrontal cortex, is a portion of the limbic thalamus central to reward processing. Vasopressin and the related neuropeptide oxytocin mediate pair-bonding in prairie voles, at least in part through their actions on reward structures (Gingrich et al., 2000; Insel and Young, 2001; Young et al., 2001): one might reasonably expect receptor expression in the MD Thal to influence pair-bonding or other forms of pro-social behaviors. Moreover, the bimodal variation (Fig. 2) within the thalamus and posterior cingulate suggests that high and low levels of V1aR expression might be associated with discrete behavioral phenotypes.

Although there were tremendous individual differences, we could find no evidence for sexually dimorphic V1aR in any brain region, despite considerable sample sizes ($P > 0.10$; Table 1). This finding is consistent with prior reports derived from smaller samples, but reinforces how anomalous it is that vasopressin seems to be a more potent activator of pair-bonding in male prairie voles (e.g., Cho et al., 1999). The absence of sex differences also suggests

that gonadal steroids are not driving individual differences. This finding is consistent with studies that have failed to find an influence of neonatal or adult castration on the pattern of V1aR (Cushing et al., 2003; Wang, personal communication). Perhaps developmental differences in adrenal steroids or neonatal environments may shape V1aR expression profiles. Neonatal exposure to adrenal steroids influences adult behavior in prairie voles (Roberts et al., 1997). Variation in maternal care has been linked to V1aR in the brains of male rats (Francis et al., 2002). Although developmental perturbations may plausibly contribute to the observed variation, there is no precedent for developmental influences on many of the most variable structures (e.g., P Cing and thalamus). Another possible source of variation lies in the architecture of the V1aR gene itself. The prairie vole promoter contains a microsatellite, or repetitive DNA sequence that tends to have extremely high mutation rates (Young et al., 1999a). We found tremendous V1aR promoter diversity in a sample from this population (Phelps et al., 2002). Analogous allelic variation has been implicated in human differences in the serotonin transporter, for example (Lesch et al., 1996; Hariri et al., 2002). A high level of heritable polymorphism in V1aR phenotype would represent a pool of variation that could facilitate the evolution of the striking species differences previously reported.

Although there were many compelling differences in the variation of individual brain regions, patterns of covariation across regions were also striking. The global pattern of covariation shows a general agreement with the developmental origins of distinct brain structures. This pattern is inconsistent with clusters produced simply by the proximity of brain structures to one another. The BST and V Pall covaried strongly; we refer to this grouping as pallidal because both are derived from the pallidal ridge (Alvarez-Bolado and Swanson, 1996). The posterior cingulate cortex and the medial amygdala form a cluster. Although the posterior cingulate is pallial, most authors now consider the medial amygdala to be subpallial (Swanson and Petrovich, 1998; Puelles et al., 2000). Nevertheless, the precursors of the medial amygdala and the pallium are adjacent during development, and share common patterns of expression for several transcription factors, including Emx-1 and Pax-6 (Smith Fernandez et al., 1998; Puelles et al., 2000). The pattern of transcription factors shared by the pallium and segments of the subpallium could potentially explain the observed covariation in V1aR expression. The olfactory, pallidal, and pallial clusters combine with the lateral septum to form a deep telencephalic cluster (Fig. 4a). Similarly, the thalamic regions coalesce to form a diencephalic cluster. In fact, the only brain region that joined a cluster of clearly unrelated regions was the central nucleus of the amygdala. This finding suggests that the regulation of V1aR expression in C Amyg is somehow modified by mechanisms not shared by other regions of the telencephalon. Of interest, in a study of maternal environments on adult rat V1aR patterns, only C Amyg expression was linked to neonatal social experience (Francis et al., 2002). In any case, we cannot confidently suggest a cause for the C Amyg pattern of variation; we can, however, highlight it as an anomaly that deserves attention.

The finding that intraspecific variation in the expression of a single gene is structured by the developmental origins of brain regions is a novel finding. It is, however, consistent with a long tradition of using patterns of neuromodulator expression to define developmental and evolutionary homology between brain regions. Our data suggest that developmental homologies govern more than the presence or absence of a given gene product; differences among brain regions exhibit more subtle, quantitative patterns of covariation as well.

Perhaps surprisingly, regions that comprise functional circuits do not necessarily covary. The posterior cingulate did not show a particularly strong affinity for the laterodorsal thalamus, nor did the mediodorsal thalamus show an affinity for the ventral pallidum, medial amygdala, or the olfactory structures. Binding in the lateral septum was not reliably associated with the bed nucleus or the medial amygdala. Where functionally related regions did covary—as among olfactory or pallidal structures—this covariation seems easily explained by developmental homology.

The covariation of distinct regions executing quite different functions has clear evolutionary implications. Animals expressing high V1aR in the MD thalamus, for example, are more likely to express high levels of V1aR in the LD thalamus. These correlations raise the possibility of coordinated variation among behaviors related to pair-bonding and space-use. Given the tight evolutionary linkage of male home-range size and mating system (reflected, for example, in sex and species differences in hippocampal size [Sherry, 1998]), this is an intriguing possibility. Our data reveal a need to test whether intraspecific variation in V1aR can cause individual differences in social behaviors and whether correlations between brain regions lead to covariation in related behaviors.

Microarray studies have used cluster analysis to look at the coregulation of gene expression at the level of mRNA abundance by using correlations among genes to infer common transcriptional regulation. In one of the few studies we could find relating gene expression profiles to neuroanatomic boundaries and developmental homology, Zhao et al. (2001) found that brain regions that were developmentally related were more likely to share gene expression profiles. Given what is known regarding the hierarchical, combinatorial control of cell development and gene expression, hierarchical patterns of correlations among developmentally related structures seem likely to be a general phenomenon. Our data, however, are measures of functional protein expression and not of gene transcription. We previously have demonstrated that V1aR ligand binding and mRNA abundance are strongly related (Young et al., 1997), so our measures may indeed reflect changes in transcription. Nevertheless, whether the observed correlations between developmentally related structures are caused by shared mechanisms of transcriptional regulation remains to be demonstrated.

Whatever the causes of covariation in expression, the findings have implications for the investigation of individual differences. They suggest, for example, that behavioral consequences of individual differences in neurochemistry might present themselves as complex, correlated suites of traits that reflect coordinate variation across brain regions. Promoter differences in several neuromodulatory systems have been linked to individual differences in transcription and behavior (e.g., Lesch et al., 1996; Caspi et al., 2002; Hariri et al., 2002). To our knowledge, however, such behavioral variation is rarely considered in light of the developmental homology of brain systems influenced

by a particular neuromodulator. That prairie voles exhibit complex social behaviors, extraordinary diversity in V1aR binding, and patterns of marked covariation across related brain structures suggest that the species would be a fruitful model for experimental explorations of individual differences in neuroanatomy and behavior.

The extensive covariation among structures has comparable consequences for the emergence of species differences in receptor expression profiles. Because genetic correlations enable selection on one trait to drive the evolution of another (Lynch and Walsh, 1998), correlated expression raises the possibility that expression in any particular brain region is an evolutionary by-product of genetically correlated expression in another. In the rhesus macaque, for example, V1aR is densely expressed in layers IV and VI of the cingulate and insular cortex (Young et al., 1999b). Detailed immunocytochemical mapping studies have failed to detect any vasopressin-immunoreactive cells or fibers in any cortical layers (Caffé et al., 1989). However, the extensive cortical V1aR binding in the rhesus brain is continuous with the cortical binding in a small region of the subcallosal cingulate cortex, where vasopressin immunoreactive fibers are found. V1aR expression in some regions may not be functional but rather a byproduct of the limitations of transcriptional regulation. Mechanisms of gene regulation may drive the evolution of neuroanatomic patterns in which some aspects of gene expression are functional and adaptive while others are incidental consequences of "genetic hitch-hiking" driven by genetic correlations (Lynch and Walsh, 1998). Such hypotheses require that correlated patterns of expression are heritable—a prediction that could be readily tested.

In summary, our data demonstrate how population biology can inform our understanding of individual and species differences in neuroanatomy. Our model system, the prairie vole, exhibits individual differences comparable to interspecies differences. Despite this tremendous diversity, areas known to play a role in monogamous behavior show relatively low levels of variation—a pattern consistent with selection at these regions. We find covariation between brain regions reflects their developmental origins. This finding suggests that shared mechanisms of transcriptional regulation may influence the patterns of individual and species differences in neuropeptide function. This model system may prove tremendously useful for understanding the causes and consequences of natural diversity in neuropeptide systems. By studying the natural history of a neuropeptide receptor, we hope to inform future studies of how naturally occurring differences in the expression of a single gene can shape the origin and evolution of species differences in complex social behavior.

ACKNOWLEDGMENTS

The authors thank Drs. Joyce Hofman and Ed Heske of the Illinois Natural History Survey and Dr. Lowell Getz, of the University of Illinois for their expert instruction in field identification and trapping methods. The authors also thank Drs. Joyce Hofman and Larry Page of the Illinois Natural History Survey for providing field equipment used in this study. We thank Dr. Thomas Insel for his critical evaluation of our methods and data, and Drs. Hemu Nair and Walter Wilczynski for contributing their substantial neuroanatomic expertise.

LITERATURE CITED

Alvarez-Bolado G, Swanson LW. 1996. Developmental brain maps: structure of the embryonic rat brain. Amsterdam: Elsevier.

Bester-Meredith JK, Young LJ, Marler CA. 1999. Species differences in paternal behavior and aggression in Peromyscus and their associations with vasopressin immunoreactivity and receptors. Horm Behav 36:25–38.

Boyd SK. 1994. Arginine vasotocin facilitation of advertisement calling and call phonotaxis in bullfrogs. Horm Behav 28:232–240.

Brown JKM. 1994. Bootstrap hypothesis tests for evolutionary trees and other dendrograms. Proc Natl Acad Sci 91:12293–12297.

Caffé AR, Van Ryen PC, Van der Woude TP, Van Leeuwen FW. 1989. Vasopressin and oxytocin systems in the brain and upper spinal cord of Macaca fascicularis. J Comp Neurol 287:302–325.

Caspi A, McClay J, Moffitt TE, Mill J, Martin J, Craig IW, Taylor A, Poulton R. 2002. Role of genotype in the cycle of violence in maltreated children. Science 297:851–854.

Cho MM, DeVries AC, Willams JR, Carter CS. 1999. The effects of oxytocin and vasopressin on partner preferences in male and female prairie voles (Microtus ochrogaster). Behav Neurosci 113:1071–1079.

Cooper BG, Manka TF, Mizumori SJY. 2001. Finding your way in the dark: the retrosplenial cortex contributes to spatial memory and navigation without visual cues. Behav Neurosci 115:1012–1028.

Cushing BS, Okorie U, Young LJ. 2003. The effects of early exposure of testosterone on the subsequent response of adult male prairie voles to arginine vasopressin. J Neuroendocrinol (in press).

Englemann M, Landgraf R. 1994. Microdialysis administration of vasopressin into the septum improves social recognition in brattleboro rats. Physiol Behav 55:145–149.

Ferris CF, Albers HE, Wesolowski SM, Goldman B, Leeman S. 1984. Vasopressin injected into the hypothalamus triggers a stereotypic behavior in golden hamsters. Science 224:521–523.

Ferris CF, Melloni RH, Koppel G, Perry KW, Fuller RW, Delville Y. 1997. Vasopressin/serotonin interactions in the anterior hypothalamus control aggressive behavior in golden hamsters. J Neurosci 17:4331–4340.

Francis DD, Young LJ, Meaney MJ, Insel TR. 2002. Naturally occurring differences in maternal care are associated with the expression of oxytocin and vasopressin (V1a) receptors: gender differences. J Neuroendocrinol 14:349–353.

Gingrich B, Liu Y, Cascio C, Wang Z, Insel TR. 2000. Dopamine D2 receptors in the nucleus accumbens are important for social attachment in female prairie voles (Microtus ochrogaster). Behav Neurosci 114:173–183.

Goodson J. 1998. Territorial aggression and dawn song are modulated by septal vasotocin and vasoactive intestinal polypeptide in male field sparrows (*Spizella pusilla*). Horm Behav 34:67–77.

Goodson JL, Bass AH. 2000. Forebrain peptides modulate sexually polymorphic vocal circuitry. Nature 403:769–772.

Goodson JL, Bass AH. 2001. Social behavior functions and related anatomical characteristics of vasotocin/vasopressin systems in vertebrates. Brain Res Rev 35:246–265.

Hariri AR, Mattay VS, Tessitore A, Kolachana B, Fera F, Goldman D, Egan MF, Weinberger DR. 2002. Serotonin transporter genetic variation and the response of the human amygdala. Science 297:400–403.

Hoffmeister DF. 1989. Mammals of Illinois. Champaign, IL: University of Illinois Press.

Insel TR, Young LJ. 2001. Neurobiology of social attachment. Nat Neurosci 2:129–136.

Insel TR, Wang Z, Ferris CF. 1994. Patterns of brain vasopressin receptor distribution associated with social organization in microtine rodents. J Neurosci 14:5381–5392.

Kirkpatrick B, Carter CS, Newman SW, Insel TR. 1994a. Axon-sparing lesions of the medial nucleus of the amygdala decrease affiliative behaviors in the prairie vole (*M. ochrogaster*): behavioral and anatomical specificity. Behav Neurosci 108:501–513.

Kirkpatrick B, Kim JW, Insel TR. 1994b. Limbic system *fos* expression associated with paternal behavior. Brain Res 658:112–118.

Lesch K-P, Bengel D, Heils A, Sabol SZ, Greenberg BD, Petri S, Benjamin J, Mueller CR, Hamer DH, Murphy D. 1996. Association of anxiety-related traits with a polymorphism in the serotonin transporter gene regulatory region. Science 274:1527–1531.

Lynch M, Walsh B. 1998. Genetics and analysis of quantitative traits. Sunderland, MA: Sinauer.

Paxinos G, Watson C. 1998. The rat brain in stereotaxic coordinates. New York: Academic Press.

Phelps SM, Sharer CA, Young LJ. 2002. Individual differences in vasopressin V1a receptors, promoter structure and social behavior. Soc Neurosci Abstr. 89.1.

Pitkow LJ, Sharer CA, Ren X, Insel TR, Terwilliger EF, Young LJ. 2001. Facilitation of affiliation and pair-bond formation by vasopressin receptor gene transfer into the ventral forebrain of a monogamous vole. J Neurosci 21:7392–7396.

Puelles L, Kuwana E, Puelles E, Bulfone A, Shimamura K, Keleher J, Smiga S, Rubenstein J. 2000. Pallial and subpallial derivatives in the embryonic chick and mouse telencephalon, traced by the expression of the genes Dlx-2, Emx-1, Nkx-2.1, Pax-6, and Tbr-1. J Comp Neurol 424:409–438.

Roberts RL, Zullo AS, Carter CS. 1997. Sexual differentiation in prairie voles: the effects of corticosterone and testosterone. Physiol Behav 62:1379–1383.

Sherry DF. 1998. The ecology and neurobiology of spatial memory. In: Deukas R, editor. Cognitive Ecology. Chicago: University of Chicago Press.

Smith Fernandez A, Pieau C, Repérant J, Boncinelli E, Wassef M. 1998. Expression of the Emx-1 and Dlx-1 homeobox genes define three molecularly distinct domains in the telencephalon of mouse, chick, turtle and frog embryos: implications for the evolution of telencephalic subdivisions in amniotes. Development 125:2099–2111.

Swanson L, Petrovich G. 1998. What is the amygdala? TINS 21:323–331.

Wang Z, Ferris CF, DeVries GJ. 1994. Role of septal vasopressin innervation in paternal behavior in prairie voles (*Microtus ochrogaster*). Proc Natl Acad Sci U S A 91:400–404.

Wang Z, Toloczko D, Young LJ, Moody K, Newman JD, Insel TR. 1997. Vasopressin in the forebrain of common marmosets (*Callithrix jacchus*): studies with in situ hybridization, immunocytochemistry and receptor autoradiography. Brain Res 768:147–156.

Whishaw IQ, Maaswinkel H, Gonzalez CLR, Kolb B. 2001. Deficits in allothetic and idiothetic spatial behavior in rats with posterior cingulate cortex lesions. Behav Brain Res 118:67–76.

Winslow J, Hastings N, Carter CS, Harbaugh C, Insel. T. 1993. A role for central vasopressin in pair bonding in monogamous prairie voles. Nature 365:545–548.

Young LJ. 1999. Oxytocin and vasopressin receptors and species-typical social behaviors. Horm Behav 36:212–221.

Young LJ, Winslow JT, Nilsen R, Insel TR. 1997. Species differences in V1a receptor gene expression in monogamous and non-monogamous voles: behavioral consequences. Behav Neurosci 111:599–605.

Young LJ, Nilsen R, Waymire KG, MacGregor GR, Insel TR. 1999a. Increased affiliative response to vasopressin in mice expressing the vasopressin receptor from a monogamous vole. Nature 400:766–768.

Young LJ, Toloczko D, Insel TR. 1999b. Localization of vasopressin (V1a) receptor binding and mRNA in the rhesus monkey brain. J Neuroendocrinol 11:291.

Young LJ, Lim MM, Gingrich B, Insel TR. 2001. Cellular mechanisms of social attachment. Horm Behav 40:133–138.

Zhao X, Lein ES, He A, Smith SC, Aston C, Gage FH. 2001. Transcriptional profiling reveals strict boundaries between hippocampal subregions. J Comp Neurol 441:187–196.